

Gravitational wave from rotating neutron star

Shailesh K. Singh¹, S. K. Biswal¹, M. Bhuyan¹, T. K. Jha² and S. K. Patra¹

¹*Institute of Physics, Bhubaneswar-05, India.*

²*Department of Physics, BITS Pilani, K K Birla Goa.*

(Dated: July 8, 2021)

Using the nuclear equation of states for a large variety of relativistic and non-relativistic force parameters, we calculate the static and rotating masses and radii of neutron stars. From these equation of states, we also evaluate the properties of rotating neutron stars, such as rotational and gravitational frequencies, moment of inertia, quadrupole deformation parameter, rotational ellipticity and gravitational wave strain amplitude. The estimated gravitational wave strain amplitude of the star is found to be $\sim 10^{-23}$.

PACS numbers: 95.85.Sz, 26.60.Kp, 97.60.Jd, 04.25.-g

I. INTRODUCTION

Gravitational wave is a fundamental feature of elliptically deformed pulsars. It is produced due to the axially asymmetry of the system. This is one of the unique source of informations which can resolve most of the mystery of the stellar objects. About 96 percent mass-energy of the Universe has no charge, so the major fact about Universe can be revealed from the gravitational wave (GW). However, it is unlike to detect easily as it is done in electromagnetic wave, which is originated from charge sources [1]. Thus, the detection of gravitational waves is hard due to its low frequency and background sources.

There are experimental set up using ground based detectors, which are specially designed for the measurement of gravitational waves amplitude, such as the Laser Interferometer Gravitational wave Observatory science collaboration (LIGO) and the German-British Gravitational wave Detectors (GEO600). The sensitivity of the detection is increased by the merger of these data and the upper limit of the gravitational wave amplitude is observed to be $\sim 2.6 \times 10^{-25}$ for pulsar PSR I1603-7202 and the ellipticity of pulsar PSR I2124-3358 is found to be less than 10^{-6} [2]. Some other spaced based detectors like Laser Interferometer Antenna (LISA) is designed for detecting the low frequency (0.03 mHz to 0.1 Hz) gravitational waves [3] and space based Cosmic Visions 2015-2025 is in plan to orbiting the sun like LISA to gain more sensitiveness towards the low frequency gravitational wave signals [1].

The neutron star (NS) and black holes are formed from the gravitational collapse of a highly evolved star or core collapse of an accreting white dwarf. The neutron star is the final stage of the evolving star and then it fails to collapse and form a black hole due to gravity. Rotating deform neutron star emits gravitational waves which carry the information about the neutron star (NS). Therefore, it is very important to discuss the upper limit of GW amplitude, rotational frequency ν_r , quadrupole moment Φ_{22} and ellipticity ϵ of a neutron star predicted by various theoretical models. The static mass of the NS compared with recently observed data [4], which is quite massive than the earlier measured mass from the neutron star pulsar PSR 1913+16 ($M = 1.144M_\odot$) [5]. Those equation of states (EOS) give the mass of Taylor et al. [5] fails to reproduce the maximum mass of $(1.97 \pm 0.04)M_\odot$ [4]. Thus,

to get a larger mass, one needs a stiff EOS, which again oppose the softer EOS of kaon production [6, 7]. To make such a model in the same footing, extra interactions are needed as it is done in the construction of G1 and G2 parametrizations [8–10]. In the present paper, we have used 20 different force parameters for both non-relativistic and relativistic mean field equation of states (EOS) to calculate the gravitational wave strain amplitude of rotating neutron stars.

The paper starts with a short introduction in Sec. I. The formalisms of Skyrme Hartree-Fock (SHF) and Relativistic Mean Field (RMF) theory are presented in Sec.II. In this section we have outlined the Hamiltonian, Lagrangian and equation of states (EOS) for non-relativistic and relativistic formalisms. The SHF and RMF parameter sets are also tabulated in this section. The calculated results of pressure and energy obtained from these forces are discussed in Sec. III. Here, the masses of the neutron stars and their respective radii both in static and rotating frames are estimated and then used these observables to estimate the gravitational wave strain amplitude. The related quantities like rotational frequency ν_r , quadrupole moment Φ_{22} and ellipticity ϵ of rotating neutron star also calculated. The paper is summarized in Sec. IV.

II. THEORETICAL FORMALISMS

A. Skyrme Hartree-Fock (SHF) method

There are many known parametrizations of Skyrme interaction which reproduce the experimental data for ground state properties of finite nuclei [11, 12] as well as the properties of infinite nuclear matter upto high density [13]. The general form of the Skyrme effective interaction can be expressed as a density functional \mathcal{H} with some empirical parameters [12, 14, 15]:

$$\mathcal{H} = \mathcal{K} + \mathcal{H}_0 + \mathcal{H}_3 + \mathcal{H}_{eff} + \dots, \quad (1)$$

where \mathcal{K} is the kinetic energy, \mathcal{H}_0 the zero range, \mathcal{H}_3 the density dependent and \mathcal{H}_{eff} the effective-mass dependent terms, which are relevant for calculating the properties of nuclear matter. More details can be found in Refs. [12, 14, 15]. These are functions of 9 parameters t_i , x_i ($i = 0, 1, 2, 3$) and η are

given as

$$\begin{aligned}\mathcal{H}_0 &= \frac{1}{4}t_0 [(2+x_0)\rho^2 - (2x_0+1)(\rho_p^2 + \rho_n^2)], \\ \mathcal{H}_3 &= \frac{1}{24}t_3\rho^\eta [(2+x_3)\rho^2 - (2x_3+1)(\rho_p^2 + \rho_n^2)], \\ \mathcal{H}_{eff} &= \frac{1}{8}[t_1(2+x_1) + t_2(2+x_2)]\tau\rho \\ &\quad + \frac{1}{8}[t_2(2x_2+1) - t_1(2x_1+1)](\tau_p\rho_p + \tau_n\rho_n).\end{aligned}$$

The kinetic energy $\mathcal{K} = \frac{\hbar^2}{2m}\tau$, a form used in the Fermi gas model for non-interacting Fermions. The total nucleon number density $\rho = \rho_n + \rho_p$, the kinetic energy density $\tau = \tau_n + \tau_p$.

The standard form of the Skyrme effective interaction can be expressed as [15–17]:

$$\begin{aligned}V_{eff}(r_1, r_2) &= t_0(1+x_0P_\sigma)\delta(r) \\ &\quad + \frac{1}{2}t_1(1+x_1P_\sigma) [\mathbf{P}'^2\delta(r) + \delta(r)\mathbf{P}^2] \\ &\quad + t_2(1+x_2P_\sigma)\mathbf{P}' \cdot \delta(r)\mathbf{P} \\ &\quad + \frac{t_3}{6}(1+x_3P_\sigma)(\rho(\mathbf{R}))^\gamma\delta(r).\end{aligned}$$

Here, $r = r_1 - r_2$, $R = \frac{1}{2}(r_1 + r_2)$, $P = \frac{1}{2i}(\nabla_1 - \nabla_2)$ and $\sigma = \sigma_1 + \sigma_2$. The main advantage of the Skyrme density functional is that it allows the analytical expression for all variables explaining the infinite nuclear matter characteristics. The general expression for the energy per particle of asymmetric nuclear matter (ANM) in terms of energy density ε and number density ρ is given by [15, 18]:

$$\begin{aligned}\frac{E}{A}(Y_p, \rho) &= \frac{\varepsilon(\rho)}{\rho} = \frac{3}{10}\frac{\hbar^2}{2m}\left(\frac{3\pi^2}{2}\right)^{2/3}\rho^{2/3}F_{5/3} \\ &\quad + \frac{1}{8}t_0\rho^2[2(x_0+2) - (2x_0+1)F_2] \\ &\quad + \frac{1}{48}t_3\rho^{(\sigma+1)}[2(x_3+2) - (2x_3+1)F_2] \\ &\quad + \frac{3}{40}\left(\frac{3\pi^2}{2}\right)^{2/3}\rho^{5/3}[t_1(x_1+2) + t_2(x_2+2)]F_{8/3} \\ &\quad + \frac{3}{80}\left(\frac{3\pi^2}{2}\right)^{2/3}\rho^{5/3}[t_2(2x_2+1) - t_1(2x_1+1)]F_{8/3}\end{aligned}$$

with the asymmetric factor,

$$F_m(Y_p) = 2^{m-1} [Y_p^m + (1 - Y_p^m)].$$

The term Y_p is adopted in place of isospin to define the asymmetry of the infinite nuclear matter, which is common notation in astrophysics. The analytical form of the pressure density

can be expressed as:

$$\begin{aligned}P(Y_p, \rho) &= \frac{1}{5}\frac{\hbar^2}{2m}\left(\frac{3\pi^2}{2}\right)^{2/3}\rho^{5/3}F_{5/3} \\ &\quad + \frac{1}{8}t_0\rho^2[2(x_0+2) - (2x_0+1)F_2] \\ &\quad + \frac{1}{48}t_3\rho^{(\sigma+2)}[2(x_3+2) - (2x_3+1)F_2] \\ &\quad + \frac{3}{40}\left(\frac{3\pi^2}{2}\right)^{2/3}\rho^{8/3}[t_1(x_1+2) + t_2(x_2+2)]F_{8/3} \\ &\quad + \frac{3}{8}\left(\frac{3\pi^2}{2}\right)^{2/3}\rho^{8/3}[t_2(2x_2+1) - t_1(2x_1+1)]F_{8/3}.\end{aligned}$$

The symmetry energy $E_{sym}(\rho)$, slope parameter $L(\rho)$, symmetry incompressibility $K_{sym}(\rho)$ and incompressibility at saturation $K_0(\rho_0)$ can be derived from the energy density, which are explicitly given in Refs. [13]. The 13 Skyrme parameter sets used in the present calculations are SGII [19], SkM* [20], RATP [21], SLy23a [15], SLy23b [15], SLy4 [22], SLy5 [22], SKT1 [23], SKT2 [23], KDE0v1 [24], LNS [25], NRAPR [26], SkMP [27] and displayed in Table I.

B. Relativistic mean field (RMF) formalism

In principle, one should use quantum chromodynamics (QCD), the fundamental theory of strong interaction, for the complete description of EOS. But it cannot be used to describe hadronic matter due to its non-perturbative properties. A major breakthrough occurred when the concept of effective field theory (EFT) was introduced and applied to low energy QCD [28]. The degrees of freedom in this theory are nucleons interacting through the exchange of iso-scalar scalar σ , iso-scalar vector ω , iso-vector-vector ρ and the pseudoscalar π mesons. The nucleons are considered as Dirac particle moving in classical meson fields. The contribution of π meson is zero at mean field level, due to pseudo-spin nature. The chiral effective Lagrangian (E-RMF) proposed by Furnstahl, Serot and Tang [8–10] is the extension of the standard relativistic mean field (RMF) theory [29, 30] with the addition of non-linear scalar-vector and vector-vector self interaction. This Lagrangian includes all the non-renormalizable couplings consistent with the underlying symmetries of QCD. Applying the naive dimensional analysis [31, 32] and the concept of naturalness one can expand the nonlinear Lagrangian and organize it in increasing powers of the fields and their derivatives and truncated at given level of accuracy [33–35]. In practice, to get a reasonable result, one needs the Lagrangian up to 4th order of interaction. Thus, the considered model involves the nucleons interacting through the mesons. The truncated Lagrangian which includes the terms up to the fourth order is

given by

$$\begin{aligned}
\mathcal{L} = & \bar{\Psi}_B (i\gamma^\mu D_\mu - m_B + g_{\sigma B}\sigma) \Psi_B + \frac{1}{2}\partial_\mu\sigma\partial^\mu\sigma \\
& - m_\sigma^2\sigma^2 \left(\frac{1}{2} + \frac{\kappa_3}{3!} \frac{g_{\sigma B}\sigma}{m_B} + \frac{\kappa_4}{4!} \frac{g_{\sigma B}^2\sigma^2}{m_B^2} \right) - \frac{1}{4}\Omega_{\mu\nu}\Omega^{\mu\nu} \\
& + \frac{1}{2} \left(1 + \eta_1 \frac{g_{\sigma B}\sigma}{m_B} + \frac{\eta_2}{2} \frac{g_{\sigma B}^2\sigma^2}{m_B^2} \right) m_\omega^2\omega_\mu\omega^\mu \\
& - \frac{1}{4}R_{\mu\nu}^a R^{a\mu\nu} + \left(1 + \eta_\rho \frac{g_{\sigma B}\sigma}{m_B} \right) \frac{1}{2}m_\rho^2\rho_\mu^a\rho^{a\mu} \\
& + \frac{1}{4!}\zeta_0 g_{\omega B}^2 (\omega_\mu\omega^\mu)^2. \tag{2}
\end{aligned}$$

The subscript $B = n, p$ denotes for nucleons. The terms in eqn. (2) with the subscript B should be interpreted as sum over the states of nucleons. The covariant derivative D_μ is

defined as

$$D_\mu = \partial_\mu + ig_{\omega B}\omega_\mu + ig_{\phi B}\phi_\mu + ig_{\rho B}I_{3B}\tau^a\rho_\mu^a, \tag{3}$$

whereas $R_{\mu\nu}^a$, and $\Omega_{\mu\nu}$ are the field tensors

$$R_{\mu\nu}^a = \partial_\mu\rho_\nu^a - \partial_\nu\rho_\mu^a + g_\rho\epsilon_{abc}\rho_\mu^b\rho_\nu^c, \tag{4}$$

$$\Omega_{\mu\nu} = \partial_\mu\omega_\nu - \partial_\nu\omega_\mu, \tag{5}$$

where m_B denotes the baryon and m_σ , m_ω , m_ρ are the masses assigned to the meson fields. Using this Lagrangian, we derive the equation of motion and solved it in the mean field approximation self consistently. Here, the meson fields are replaced by their classical expectation values. The field equations for σ , ω and ρ -meson are given by

$$m_\sigma^2 \left(\sigma_0 + \frac{g_{\sigma B}\kappa_3}{2m_B}\sigma_0^2 + \frac{g_{\sigma B}^2\kappa_4}{6m_B^2}\sigma_0^3 \right) - \frac{1}{2}m_\rho^2\eta_\rho \frac{g_\sigma}{m_B}\rho_0^2 - \frac{1}{2}m_\omega^2 \left(\eta_1 \frac{g_{\sigma B}}{m_B} + \eta_2 \frac{g_{\sigma B}^2}{m_B^2}\sigma_0 \right) \omega^2 = \sum_B g_{\sigma B}\rho_{SB}, \tag{6}$$

$$m_\omega^2 \left(1 + \frac{\eta_1 g_\sigma}{m_B}\sigma_0 + \frac{\eta_2 g_\sigma^2}{2m_B^2}\sigma_0^2 \right) \omega_0 + \frac{1}{6}\zeta_0 g_{\omega B}^2 \omega_0^3 = \sum_B g_{\omega B}\rho_B, \tag{7}$$

and

$$m_\rho^2 \left(1 + \frac{g_{\sigma B}\eta_\rho}{m_B}\sigma_0 \right) \rho_{03} = \sum_B g_{\rho B}I_{3B}\rho_B. \tag{8}$$

For a baryon species, the scalar density, ρ_{SB} , and baryon density (ρ_B) are

$$\rho_{SB} = \frac{2J_B + 1}{2\pi^2} \int_0^{k_B} \frac{k^2 dk}{E_B^*} \tag{9}$$

and

$$\rho_B = \frac{2J_B + 1}{2\pi^2} \int_0^{k_B} k^2 dk, \tag{10}$$

where $E_B^* = \sqrt{k_B^2 + m_B^{*2}}$ is the effective energy and J_B and I_{3B} are the spin and isospin projection of baryon B , the quantity k_B is the Fermi momentum for the baryon, $m^* = m_B - g_{\sigma B}\sigma$ is the effective mass, which is solved self-consistently. After obtaining the self-consistent fields, the pressure \mathcal{P} and total energy density ε for a given baryon density are

$$\begin{aligned}
\mathcal{P} = & \frac{\gamma}{3(2\pi)^3} \int_0^{k_B} d^3k \frac{k^2}{E_B^*(k)} + \frac{1}{4!}\zeta_0 g_{\omega B}^2 \omega_0^4 + \frac{1}{2} \left(1 + \eta_1 \frac{g_{\sigma B}\sigma_0}{m_B} + \frac{\eta_2}{2} \frac{g_{\sigma B}^2\sigma_0^2}{m_B^2} \right) m_\omega^2 \omega_0^2 \\
& - m_\sigma^2 \sigma_0^2 \left(\frac{1}{2} + \frac{\kappa_3 g_{\sigma B}\sigma_0}{3!m_B} + \frac{\kappa_4 g_{\sigma B}^2\sigma_0^2}{4!m_B^2} \right) + \frac{1}{2} \left(1 + \eta_\rho \frac{g_{\sigma B}\sigma_0}{m_B} \right) m_\rho^2 \rho_0^2 + P_l, \tag{11}
\end{aligned}$$

and

$$\begin{aligned} \mathcal{E} = & \frac{\gamma}{(2\pi)^3} \int_0^{k_B} d^3k E_B^*(k) + \frac{1}{8} \zeta_0 g_{\omega B}^2 \omega_0^4 + \frac{1}{2} \left(1 + \eta_1 \frac{g_{\sigma B} \sigma_0}{m_B} + \frac{\eta_2}{2} \frac{g_{\sigma B}^2 \sigma_0^2}{m_B^2} \right) m_{\omega B}^2 \omega_0^2 \\ & + m_{\sigma B}^2 \sigma_0^2 \left(\frac{1}{2} + \frac{\kappa_3 g_{\sigma B} \sigma_0}{3! m_B} + \frac{\kappa_4 g_{\sigma B}^2 \sigma_0^2}{4! m_B^2} \right) + \frac{1}{2} \left(1 + \eta_\rho \frac{g_{\sigma B} \sigma_0}{m_B} \right) m_\rho^2 \rho_0^2 + \varepsilon_l, \end{aligned} \quad (12)$$

here, γ is the spin degeneracy ($\gamma=2$ for pure neutron matter and $\gamma=4$ for symmetric nuclear matter), P_l and ε_l are lepton pressure and energy density, respectively. For the stability of neutron star in which the strongly interacting particles are baryons, the composition is determined by the requirements of charge neutrality and β -equilibrium conditions under the weak processes $B_1 \rightarrow B_2 + l + \bar{\nu}_l$ and $B_2 + l \rightarrow B_1 + \nu_l$. After deleptonization, the charge neutrality condition yields

$$q_{\text{tot}} = \sum_B q_B (2J_B + 1) k_B^3 / (6\pi^2) + \sum_{l=e,\mu} q_l k_l^3 / (3\pi^2) = 0, \quad (13)$$

where q_B corresponds to the electric charge of baryon species B and q_l corresponds to the electric charge of lepton species l . Since the time scale of a star is effectively infinite compared to the weak interaction time scale, weak interaction violates strangeness conservation. The strangeness quantum number is therefore not conserved in a star and the net strangeness is determined by the condition of β -equilibrium, which for baryon B is given by $\mu_B = b_B \mu_n - q_B \mu_e$, where μ_B is the chemical potential of baryon B and b_B its baryon number. Thus the chemical potential of any baryon can be obtained from the two independent chemical potentials μ_n and μ_e for neutron and electron, respectively. The lepton Fermi momenta are the positive real solutions of $(k_e^2 + m_e^2)^{1/2} = \mu_e$ and $(k_\mu^2 + m_\mu^2)^{1/2} = \mu_\mu = \mu_e$. The equilibrium composition of the star is obtained by putting the β -equilibrium with the charge neutrality condition Eqn. (13) at a given total baryonic density $\rho = \sum_B (2J_B + 1) k_B^3 / (6\pi^2)$; the baryon effective masses are obtained self-consistently. In our calculation, we have taken 7 well established parameter sets such as: G2 [9], G1 [9], NL3 [36], TM1 [37], FSU [38], L1 [29], SH [39]. These all parameters along with their saturation properties are given in Table I.

C. Stellar Equations

In the interior part of neutron star, the neutron chemical potential exceeds the combined masses of the proton and electron. Therefore, asymmetric matter with an admixture of electrons rather than pure neutron matter, is a more likely composition of matter in neutron star interiors. The concentrations of neutrons, protons and electrons can be determined from the condition of β -equilibrium $n \leftrightarrow p + e + \bar{\nu}$ and from charge neutrality, assuming that neutrinos are not degenerate. Here n , p , ν have their usual meaning of neutron, proton and neutrino, respectively. In momentum conservation condition

$\nu_n = \nu_p + \nu_e$, $n_p = n_e$, where $\nu_n = \mu_n - g_\omega V_0 + \frac{1}{2} g_\rho b_0$ and $\nu_p = \mu_p - g_\omega V_0 - \frac{1}{2} g_\rho b_0$ with $\mu_n = \sqrt{(k_{fn}^2 + M_n^{*2})}$ and $\mu_p = \sqrt{(k_{fp}^2 + M_p^{*2})}$ are the chemical potential, and k_{fn} and k_{fp} are the Fermi momentum for neutron and proton, respectively. Imposing this conditions, in the expressions of \mathcal{E} and \mathcal{P} , we evaluate \mathcal{E} and \mathcal{P} as a function of density. To calculate the star structure, we use the Tolman-Oppenheimer-Volkoff (TOV) equations for the structure of a relativistic spherical and static star composed of a perfect fluid were derived from Einstein's equations [40], where the pressure and energy densities are only the input ingredients. The TOV equation is given by [40]:

$$\frac{d\mathcal{P}}{dr} = -\frac{G}{r} \frac{[\mathcal{E} + \mathcal{P}] [M + 4\pi r^3 \mathcal{P}]}{(r - 2GM)}, \quad (14)$$

$$\frac{dM}{dr} = 4\pi r^2 \mathcal{E}, \quad (15)$$

with G as the gravitational constant and $M(r)$ as the enclosed gravitational mass. We have used $c = 1$, the velocity of light. Given the \mathcal{P} and \mathcal{E} , these equations can be integrated from the origin as an initial value problem for a given choice of central energy density. The value of r ($= R$), where the pressure vanishes defines the surface of the star. Another realistic approximation that when neutron star is rotating with static, axial symmetric, space-time, the time translational invariant and axial-rotational invariant metric in spherical polar coordinate (t, r, θ, ϕ) can be written as:

$$\begin{aligned} ds^2 = & -e^{2\nu} dt^2 + e^{2\alpha} (dr^2 + r^2 d\theta^2) \\ & + e^{2\beta} r^2 \sin^2 \theta (d\phi - \omega dt)^2, \end{aligned} \quad (16)$$

where the metric functions ν , α , β , ω depend only on r and θ . For a perfect fluid, the energy momentum tensor can be given by:

$$T^{\mu\nu} = P g^{\mu\nu} + (\mathcal{P} + \mathcal{E}) u^\mu u^\nu, \quad (17)$$

with the four-velocity

$$u^\mu = \frac{e^{-\nu}}{\sqrt{1 - v^2}} (1, 0, 0, \Omega), \quad (18)$$

here

$$v = (\Omega - \omega) r \sin \theta e^{\beta - \nu}, \quad (19)$$

is the proper velocity relative to an observer with zero angular velocity and Ω is the angular velocity of the star measured from infinity. Now, we can compute the Einstein field equation given by

$$R_{\mu\nu} - \frac{1}{2}g_{\mu\nu}R = 8\pi T_{\mu\nu}, \quad (20)$$

where $R_{\mu\nu}$ is Ricci tensor and R is the scalar curvature. From this, we can solve the equation of motion for metric function:

$$\Delta [\rho e^\zeta] = S_\rho(r, \mu), \quad (21)$$

$$\left(\Delta + \frac{1}{r} \frac{\partial}{\partial r} - \frac{1}{r^2} \mu \frac{\partial}{\partial r} \right) \gamma e^\zeta = S_\gamma(r, \mu), \quad (22)$$

$$\left(\Delta + \frac{2}{r} \frac{\partial}{\partial r} - \frac{2}{r^2} \mu \frac{\partial}{\partial r} \right) \omega e^{\frac{\gamma-2\rho}{2}} = S_\omega(r, \mu), \quad (23)$$

where $\gamma = \beta + v$, $\rho = v - \beta$ and $\mu = \cos\theta$. The right hand side of equations are the source terms. One can find more details about these equations in Ref. [41]. We can put the limit on the maximum rotation i.e. Kepler frequency Ω_k , by the onset of mass shedding from equator of the star. The final expression for Ω_k , in general relativistic formalism is given as:

$$\Omega_K = \omega + \frac{\omega'}{2\psi'} + e^{v-\beta} \left[\frac{1}{R^2} \frac{v'}{\psi'} + \left(\frac{e^{\beta-v}\omega'}{2\psi'} \right)^2 \right]^{\frac{1}{2}}, \quad (24)$$

where $\psi = \beta' + \frac{1}{R}$ and the prime denotes the differentiation with respect to the radial coordinate. For the calculation of rotational neutron star properties like mass, radius, rotational frequency, we used the well established rotational neutron star (RNS) code, which is written by Stergioulas [42, 43].

D. Properties of Rotating Neutron Star

We have calculated the maximum mass and radius of static and rotating neutron star by using well established RNS code. For this, we need only energy and pressure density which will be provided by non-relativistic and relativistic models of equation of state. Now, our aim is to calculate maximum $m = 2$ quadrupole moment for neutron star by using a chemically detailed model for the crust [44]. The relation of quadrupole moment with maximum mass M and radius R is given as:

$$\Phi_{22} = 2.4 \times 10^{38} gcm^2 \left(\frac{\sigma_{max}}{10^{-2}} \right) \left(\frac{R}{10km} \right)^{6.26} \times \left(\frac{1.4M_\odot}{M} \right)^{1.2}, \quad (25)$$

where σ_{max} is called breaking strain of the crust. In our calculation we have taken its two possible values i.e. 10^{-2} , 10^{-3} .

The quadrupole moment [Eqn. (25)] and ellipticity of the neutron star is connected to each other by a simple relation [44]:

$$\epsilon = \sqrt{\frac{8\pi}{15} \frac{\Phi_{22}}{I_{zz}}}, \quad (26)$$

where the z axis is the rotation axis and I_{zz} is the moment of inertia along the z -axis and for conventional neutron star, it is given as [45]:

$$I_{zz} = 9.2 \times 10^{44} gcm^2 \left(\frac{M}{1.4M_\odot} \right) \left(\frac{R}{10km} \right)^2 \times \left[1 + 0.7 \left(\frac{M}{1.4M_\odot} \right) \left(\frac{10km}{R} \right) \right]. \quad (27)$$

For each (non-relativistic and relativistic) parameter set we can calculate the maximum mass and radius of the neutron star and then other observables like quadrupole ellipticity and moment of inertia. The maximum rotational frequency ν_{max} of the stable rotary neutron star can be given by the simple relation [15].

$$\nu_{max} = 1.22 \times 10^3 \left(\frac{M}{M_\odot} \right)^{1/2} \left(\frac{R}{10km} \right)^{-3/2}, \quad (28)$$

Finally, we use eqns. (25 - 28) to calculate the gravitational wave strain amplitude which is presented by [2]:

$$h_0 = \frac{16\pi^2 G}{c^4} \frac{\epsilon I_{zz} \nu^2}{r}, \quad (29)$$

where r is the distance of neutron star from the earth [46].

III. RESULTS AND DISCUSSIONS

In this work, we have taken conventional static and rotating neutron star and perform the calculation for their mass and radius by using the TOV and RNS equations. The ingredients require to solve these two equations are pressure and energy density. After getting the mass and radius, we have calculated the other properties like quadrupole moment, ellipticity, moment of inertia and gravitational wave amplitude of rotating neutron star. We took the recently reported maximum mass and radius of neutron star pulsar J1614-2230 [4] and some theoretical Dirac-Bruckner Hartree-Fock results as a reference, where the star mass is $(1.97 \pm 0.04)M_\odot$. This means that an equation of state can be appreciated, if it has the capability to estimate a maximum mass at least $2.0M_\odot$.

A. Equation of State

Most of the parameters are fitted to the saturation properties of symmetric nuclear matter like binding energy per nucleon (BE/A), effective mass of nucleons, incompressibility modulus K_0 and symmetry energy E_{sym} at saturation density (ρ_0). We have shown these empirical values in Table I for both SHF and RMF parameter sets. For a general idea and to see the behaviour of these forces on binding energy per nucleon and pressure density, we have plotted figures (1) and (2). We get a stiff equation of state (EOS) for SH parameter, which is one of the oldest RMF interaction and a soft EOS for

TABLE I: The Skyrme and RMF force parameters and their nuclear matter properties, like BE/A (MeV), compressibility K_0 (MeV), nucleon effective mass ratio M^*/M , symmetry energy E_{sym} (MeV), L_{sym} (MeV), K_{sym} (MeV) at saturation density ρ_0 .

Skyrme effective interaction																
Parameter	Coupling Constants									Nuclear Saturation Properties						
	t_0	t_1	t_2	t_3	x_0	x_1	x_2	x_3	σ	ρ_0	M^*/M	BE/A	K_0	E_{sym}	L_{sym}	K_{sym}
SGII [19]	-2645.0	340.0	-41.9	15595.0	0.09	-0.06	1.43	0.06	0.17	0.16	0.79	-15.6	214.7	26.8	37.6	-145.9
SkM* [20]	-2645.0	410.0	-135.0	15595.0	0.09	0.00	0.00	0.00	0.17	0.16	0.79	-15.8	216.6	30.0	45.8	-155.9
SkMP [27]	-2372.2	503.6	57.3	12585.3	-0.16	-0.40	-2.96	-0.27	0.17	0.16	0.65	-15.6	230.9	29.9	70.3	-49.8
RATP [21]	-2160.0	513.0	121.0	11600.0	0.42	-0.36	-2.29	0.59	0.20	0.16	0.67	-16.1	239.5	29.3	32.4	-191.2
SLy23a [15]	-2490.2	489.5	-566.6	13803.0	1.13	-0.84	-1.00	1.92	0.17	0.16	0.70	-16.0	229.9	32.0	44.3	-98.2
SLy23b [15]	-2488.9	486.8	-546.4	13777.0	0.83	-0.34	-1.00	1.35	0.17	0.16	0.69	-16.0	229.9	32.0	46.0	-119.7
SLy4 [22]	-2488.9	486.8	-546.4	13777.0	0.83	-0.34	-1.00	1.35	0.17	0.16	0.69	-16.0	229.9	32.0	45.9	-119.7
SLy5 [22]	-2483.5	484.2	-556.7	13757.0	0.78	-0.32	-1.00	1.26	0.17	0.16	0.70	-16.0	229.9	32.0	48.2	-112.8
SkT1 [23]	-1794.0	298.0	-298.0	12812.6	0.15	-0.50	-0.50	0.09	0.33	0.16	1.00	-16.0	236.2	32.0	56.2	-134.8
SkT2 [23]	-1791.6	300.0	-300.0	12792.0	0.15	-0.50	-0.50	0.09	0.33	0.16	1.00	-15.9	235.7	32.0	56.2	-134.7
KDE0v1 [24]	-2553.1	411.7	-419.9	14603.6	0.65	-0.35	-0.93	0.95	0.17	0.17	0.74	-16.2	227.5	34.6	54.7	-127.1
LNS [25]	-2485.0	266.7	-337.1	14588.2	0.06	0.66	-0.96	-0.03	0.17	0.18	0.83	-15.3	210.8	33.4	61.5	-127.4
NRAPR [26]	-2719.7	417.6	-66.7	15042.0	0.16	-0.05	0.03	0.14	0.14	0.16	0.69	-15.9	225.7	32.8	59.6	-123.3

Relativistic Mean field interaction																	
Parameter	Coupling Constants									Nuclear Saturation Properties							
	g_σ	g_ω	g_ρ	k_3	k_4	ζ_0	η_1	η_2	η_r	Λ_ν	ρ_0	M^*/M	BE/A	K_0	E_{sym}	L_{sym}	K_{sym}
G2 [9]	0.84	1.02	0.76	3.25	0.63	2.64	0.65	0.11	0.39	0.00	0.15	0.66	-16.1	214.7	36.4	100.7	-7.4
G1 [9]	0.79	0.97	0.70	2.21	-10.09	3.53	0.07	-0.96	-0.27	0.00	0.15	0.60	-16.2	215.0	37.9	118.6	91.7
NL3 [36]	0.81	1.02	0.71	1.47	-5.67	0.00	0.00	0.00	0.00	0.00	0.15	0.60	-16.3	271.8	37.4	118.9	103.4
TM1 [37]	0.80	1.00	0.74	1.02	0.12	2.69	0.00	0.00	0.00	0.00	0.15	0.63	-16.3	281.1	36.9	110.6	33.8
FSU [38]	0.84	1.14	0.94	0.62	9.75	12.27	0.00	0.00	0.00	0.03	0.15	0.61	-16.3	230.0	32.6	60.4	-50.5
L1 [29]	0.76	0.93	0.00	0.00	0.00	0.00	0.00	0.00	0.00	0.00	0.19	0.56	-15.8	546.6	22.1	74.6	73.6
SH [39]	0.83	1.10	0.64	0.00	0.00	0.00	0.00	0.00	0.00	0.00	0.15	0.54	-15.8	545.0	35.0	115.6	92.8

LNS parameter, which is a successful set of SHF formalism. The rest of the EOS's for various parameter sets are between these two extremes. Our theoretical EOS for RMF and SHF results are compared with the most accepted experimental data of Danielewicz et al. [47] in Fig. 2. From the figure, it is seen that all the EOS predicted with SHF formalism passes nicely through the experimental shaded region. On the other hand, the RMF based EOS of NL3 [36], SH [39], TM1 [37] are far from the experimental observation.

However, the recently proposed G1 and G2 sets of RMF formalism very much within the experimental shaded region. These parameters not only match with the EOS of Ref. [47] but also predict the recent mass of neutron star [4]. In Fig. 3, we have shown the mass and radius trajectory of neutron star equation of state. Fig. 3(a) stands for $\frac{M_\odot}{M}$ versus central density and Fig. 3(b) is shown for $\frac{M_\odot}{M}$ as a function of neutron star radius for all the 20 force parametrizations (see below).

B. Mass and Radius of Neutron star

We noted down the maximum mass and the corresponding radius obtained from various non-relativistic and relativistic parameter sets [from TOV solution Fig. 3]. Again from the RNS code, we collected the M_{max} and R_{max} for all sets. These masses and radii are depicted in Fig. 4(a) and Fig. 4(b) for static and rotating cases, respectively. Here also, we put the maximum mass results of pulsar J1614-2230 [4] as a standard reference and compared our results.

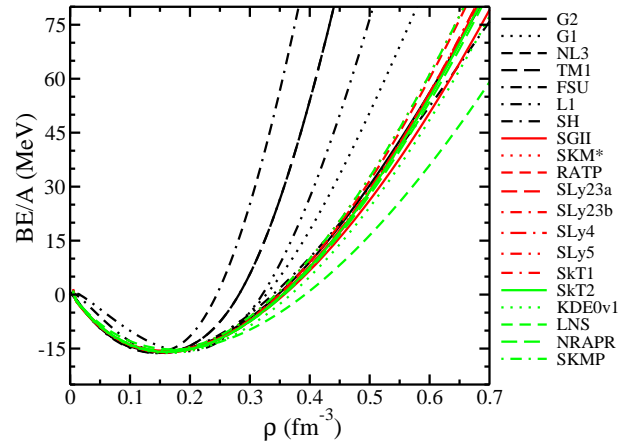


FIG. 1: Binding energy per nucleon (MeV) for symmetric nuclear matter in for non-relativistic and relativistic models with baryon density

If we compare the mass of static and rotational star, one can easily see that rotational neutron star mass is larger compare to static one for the same parameter set. As Demorest et al. [4] stated that the theoretical models should have the maximum mass more or near to $(1.97 \pm 0.04)M_\odot$. The Shapiro delay provides no information for the neutron star's radius, so we can not put any constraint on the radius of neutron star (NS).

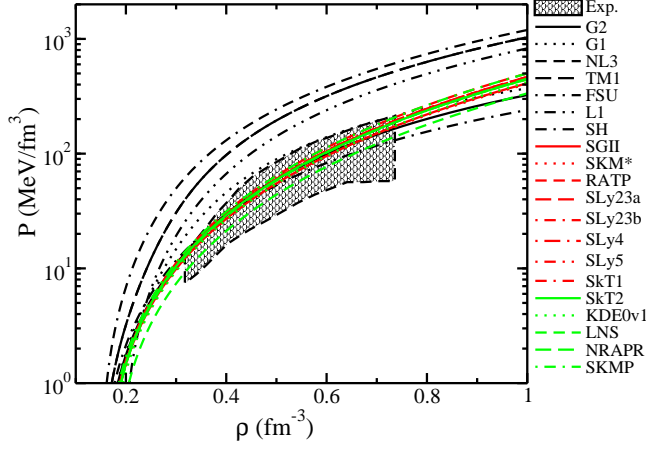


FIG. 2: Pressure density (MeV/fm^3) of symmetric nuclear matter non-relativistic and relativistic models with baryon density.

If we see the maximum mass and corresponding radius prediction of relativistic model parameter SU(2) (effective chiral model) [48], in both cases static and rotational, it is not suited to the current experimental observation [4]. The reason is the extra softness of SU(2) model, that the vector meson mass (m_ω) is generated dynamically, as a result of which the effective mass of nucleon acquires a density dependence, the effective mass increases at higher density and EOS became more softer [48]. Another non-relativistic model parameter LNS [25] which is not comfortable in static case, but it is within the cut off region for rotational NS.

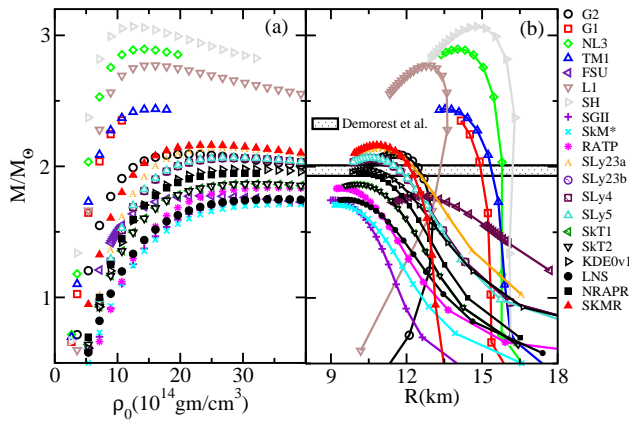


FIG. 3: Mass and radius trajectory for neutron star obtained from various parameter sets (equation of state) by using TOV equation.

We compared our calculated results with experimental data of Demorest et al. [4] which is shown by the horizontal strip in figure 3(b). From this figure, a larger number of parameter

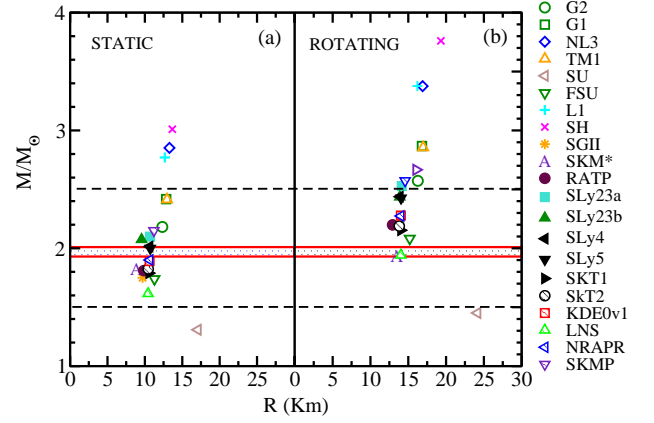


FIG. 4: Maximum mass (M/M_\odot) and radius R (km) of static and rotating neutron star in RNS model with various non-relativistic and relativistic model parameters .

sets, like FSU [38], SGII [19], SkM* [20], LNS [25], RATP [21] and SKT2 [23] are not crossing the horizontal strip, which is the experimental constraint on static slowly rotating neutron star mass ($\frac{M}{M_\odot}$) [4]. So, these parameter sets are not acceptable whole heartedly in such high density scenario and need some discussions.

(i) As we have mentioned earlier, all the relativistic and non-relativistic parameter sets are constructed at the saturation and since these are effective parameters, there is no guarantee that the extrapolation of these forces are still valid at extremely high density,

(ii) Secondly, as it is in neutron star many of the SHF forces agree well with the recent EOS experimental data of heavy ion collision [4], however these sets deviate when tested in the neutron star scenario. To reproduce the recent star mass [4] (as the masses do not lie within the experimental strip). With respect to this limit, IUFSU [49] is an extension of FSU [38] lie within the experimental constraint. For non-relativistic sets, the forces are chosen by taking into consideration their success in finite nuclei. For more descriptive study, we refer the readers go through Ref. [13], where one will get 214 SHF parameter sets and their applications to various systems.

C. Rotational and Gravitational Wave Frequency and Amplitude

Before going to discuss the gravitational wave frequency ν_{gw} , we would like to see the rotational frequency $\nu_r = \frac{\Omega_K}{2\pi}$ of neutron star. The ν_r of a NS are found to be within 7000 to 12000 Hz (except SU(2) relativistic chiral parameter) for all the considered SHF and RMF parameter sets. The maximum rotational frequency 12000 Hz is predicted by the non-relativistic SGII [19] and RATP [21] as shown in figure 5. Unlike to the rotational Keplerian frequency Ω_K , the gravitational frequency ν_{gw} is a tedious experimental exploration

[2, 3]. The calculated values of ν_{gw} obtained by various SHF and RMF parametrizations are shown in figure 6. The value of ν_{gw} is found to be almost 9 times greater than ν_r . A perfect correlation between the gravitational ν_{gw} and the rotational frequencies ν_r is shown in figure 7. From this figure, it is clear that increase of rotational results a larger emission of gravitational wave frequency ν_{gw} .

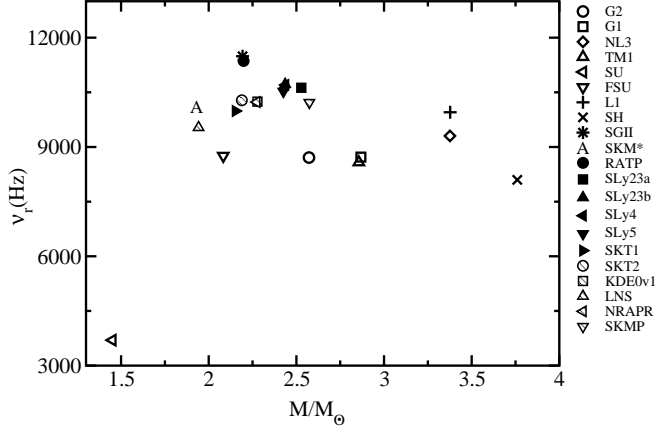


FIG. 5: The rotational wave frequency (ν_r) with maximum star mass for various parameter sets.

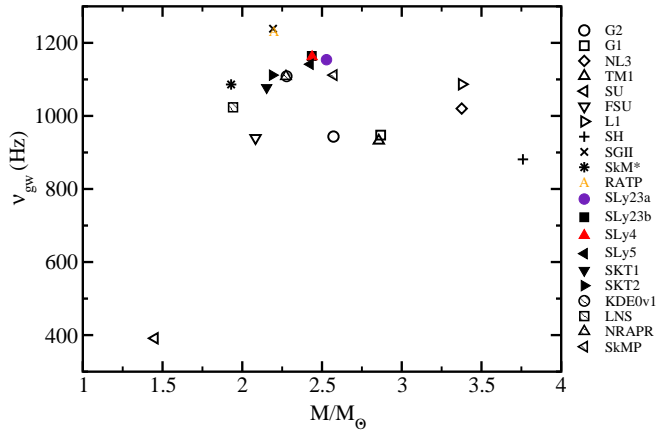


FIG. 6: Gravitational wave frequency (ν_{gw}) with maximum star mass for various parameter sets.

For a rotating neutron star, the gravitational wave amplitude h_0 is an experimental observable. We can observe it directly by specially designed experimental setup [2, 3]. The gravitational wave is generated by the rotation of an axially asymmetric neutron star. The wave strain amplitude h_0 can be measured by knowing the maximum mass and corresponding radius of a star. Its analytical feeling can be taken from the equation (29). The gravitational wave frequency ν_{gw} can be calculated by the equation (28). The relation between gravitational wave strain h_0 amplitude and frequency ν_{gw} are shown in the figure 8.

In the calculations of quadrupole moment, we have taken two set of breaking strain of the neutron star crust $\sigma =$

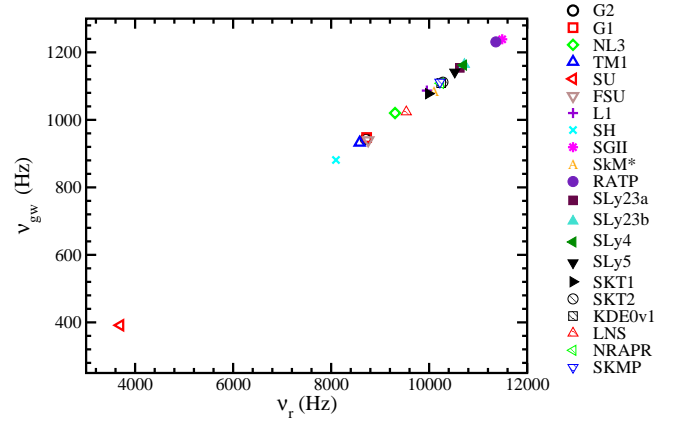


FIG. 7: Correlation between rotational frequency of neutron star and emitted gravitational wave frequency in various parameter sets.

10^{-2} , 10^{-3} and gravitational wave amplitude calculated with three sets of r (0.1, 0.2 and 0.4 kpc) which is the distance between the star and earth. These are some standard values used by earlier calculations [50]. So in this way, we have given the GW strain amplitude and frequency relation for four set of data as shown in the figure 8 along with the experimental results (for more discussion, see Ref. [50]). In our calculation, all gravitational frequencies come out more than 500 Hz, except for SU(2) model ($\nu < 300 Hz$). As we have mentioned earlier, this parameter set is unable to produce maximum mass within the experimental limit [4]. We have noticed an important point here is that the gravitational wave strain amplitude decreases with increasing the r and decreases with the value of breaking strain of neutron star crust σ .

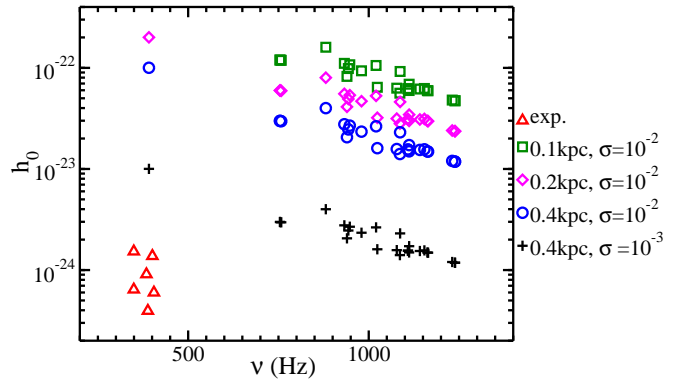


FIG. 8: Maximum gravitational wave (GW) strain amplitude h_0 with maximum possible GW frequency of rotational star.

D. Quadrupole Moment of Neutron Star

For quantitative understanding of the quadrupole moment (Φ_{22}) in different relativistic and non-relativistic models pa-

rameters, we have calculated (Φ_{22}) by using equation (25). Although, it is not valid for high frequency rotating star, but for qualitative behaviour of model parameter, we can use this approximate relation, which depends only on the mass and radius of the neutron star with the breaking strain of the neutron star crust σ . Presently, the σ value is totally uncertain and its limiting ranges are $\sigma = (10^{-5}, 10^{-2})$ [51]. In the calculations, the two chosen values of σ (10^{-2} and 10^{-3}) are taken to evaluate the quadrupole moments Φ_{22} and the results are shown in figure 9. The results are also compared with the theoretical predictions of APR and DBHF + Bonn B. The APR results shown by black line, which shows the variation of quadrupole moment of neutron star with mass, decreases continuously with M . Same trend we get in DBHF + Bonn B (red colour in Fig. 9) predictions i.e. Φ_{22} with star mass. The results with $\sigma = 10^{-3}$, match well to the APR and DBHF + Bonn B predictions, while for $\sigma = 10^{-2}$, we get very scattered values as shown in figure 9.

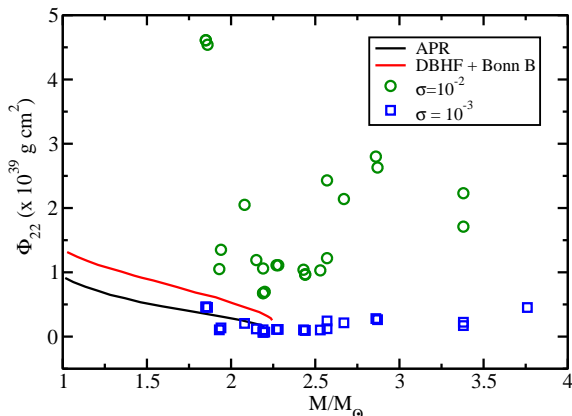


FIG. 9: Quadrupole deformation Φ_{22} with maximum mass of rotational neutron star

E. Moment of Inertia of Neutron Star

In figure 10, we have given the moment of inertia (I) of rotating neutron star. Since, inertia is a static property, it is totally depend on its mass distribution. As we know from earlier discussion in this paper, the mass of the neutron star increases with the rotational frequency ν_r . For calculating the moments of inertia (I) of the NS, we have used the maximum mass and corresponding radius and the obtained results are shown in the figure 10. The APR and DBHF + Born B results are also given in the figure for comparison.

F. Ellipticity of Neutron Star

The ellipticity of a neutron star is an important observable, which gives the structural variation of a star from its spheri-

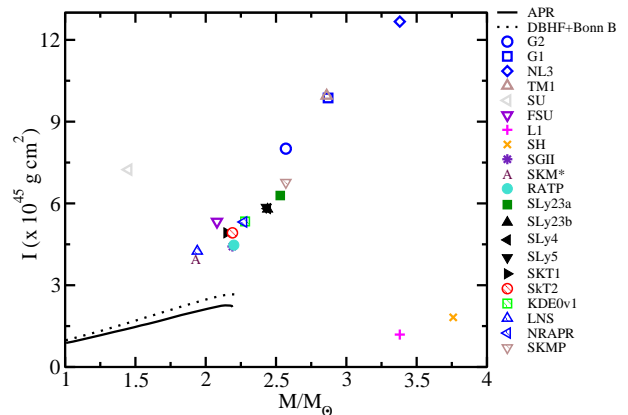


FIG. 10: Moment of inertia (I) of rotational neutron star with mass at various parameter sets.

cal shape. We can calculate it analytically by using equation (26). From this equation, ellipticity is directly related to the quadrupole moment Φ_{22} and moment of inertia (I) of the NS. We have given our calculated results obtained by all the 21 force parameters in figure 11. We have also compared our results with two theoretical models APR (black line) and DBHF + Bonn B (blue dash line) along with the two experimental results of Ref. [50] for $x = 0$ (red dotted line) and -1 (green dotted dash line). Here, we have shown the results of two sets with $\sigma = 10^{-2}$ and $\sigma = 10^{-3}$, which are shown by open circle and square in Fig. 11. As this is rotational star, the maximum mass is larger compared to slowly rotating one. If we see the results shown in the figure 11, our calculated result still matches with the earlier work at large NS mass except for SU(2) predictions [48]. Thus our predicted ellipticity of rotating neutron star using various parameter sets, where their origin are very different from each other are almost similar. The variation of the ellipticity (ϵ) obtained from various star mass is very small. This will be helpful for us to constrain the results of quadrupole moment, moment of inertia and breaking strain of the neutron star.

IV. SUMMERY AND CONCLUSIONS

In this work, we have taken the relativistic and non-relativistic models for calculation of gravitational wave strain amplitude, gravitational wave frequency, Keplerian frequency, quadrupole moment and ellipticity of rotating neutron star. We have taken maximum mass and its corresponding radius for calculating these observables. Thus, there is an indirect way to constraint the maximum mass and radius of the neutron star by these observables and vice versa. We get almost consistent results in all considered models which show the model independent predictions of the observables except for SU(2) parameter set. We found that gravitational wave strain amplitude is a function of breaking strain of neutron star crust and

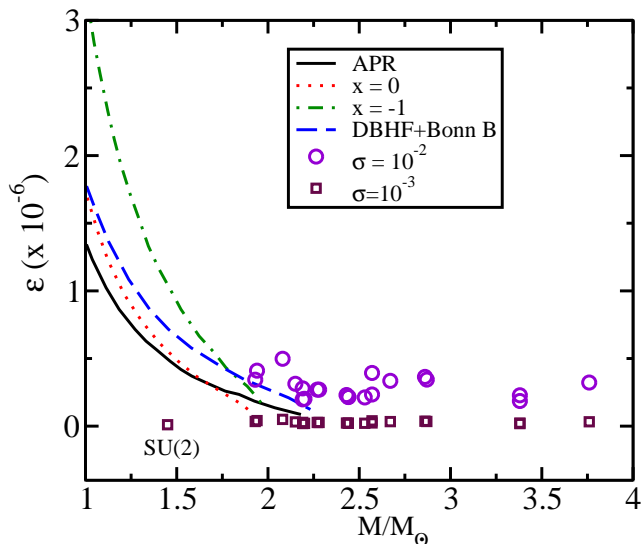


FIG. 11: Maximum rotational neutron star ellipticity with mass in different various parameter sets.

distance between the star and the earth. From our calculation, we approximate the range of the gravitational wave amplitude between 10^{-24} to 10^{-22} for rotating neutron star. The moment of inertia of the star comes around $\sim 10^{45} \text{ gcm}^2$ and the predicted range of gravitational wave frequency is in between 400 to 1280 Hz. We have calculated the rotating frequency of star and concluded that, if we increase the rotating frequency then the increment in the mass is also changes subsequently. The ellipticity of the neutron star is consistent in all the considered 21 parameter sets which will be helpful to constraint the value of quadrupole and moment of inertia of the NS and vice versa. Our results will be very helpful in the respect of the prediction of second and third generation of gravitational wave detector family.

-
- [1] B. S. Sathyaprakash and B. F. Schutz, Living Rev. Relativity **12**, 2 (2009).
- [2] B. Abbott et al., Phys. Rev. D **76**, 042001 (2007).
- [3] <http://lisa.nasa.gov/>
- [4] P. B. Demorest, T. Pennucci, S. M. Ransom, M. S. E. Roberts and J. W. T. Hessels, Nature **467**, 1081 (2010).
- [5] J. H. Taylor and J. M. Wesselberg, Astrophys. J. **345**, 434 (1989).
- [6] C. Sturm et. al., Phys. Rev. Lett. **86**, 39 (2001).
- [7] C. Fuchs, A. Faessler, E. Zabrodin and Y.-M. Zheng, Phys. Rev. Lett. **86**, 1974 (2001).
- [8] R. J. Furnstahl, B. D. Serot and H. B. Tang, Nucl. Phys. A **598**, 539 (1996).
- [9] R. J. Furnstahl, B. D. Serot and H. B. Tang, Nucl. Phys. A **615**, 441 (1997).
- [10] H. Müller and B. D. Serot, Nucl. Phys. A **606**, 508 (1996).
- [11] J. R. Stone, J. C. Miller, R. Koncewicz, P. D. Stevenson and M. R. Strayer, Phys. Rev. C **68**, 034324 (2003).
- [12] M. Bender, P.-H. Heenen and P.-G. Reinhard, Rev. Mod. Phys. **75**, 121 (2003).
- [13] M. Dutra, O. Lourenco, J. S. Sa Martins, A. Delfino, J. R. Stone and P. D. Stevenson, Phys. Rev. C **85**, 035201 (2012).
- [14] J. R. Stone and P.-G. Reinhard, Prog. Part. Nucl. Phys. **58**, 587 (2007).
- [15] E. Chabanat, P. Bonche, P. Haensel, J. Meyer and R. Schaeffer, Nucl. Phys. A **627**, 710 (1997).
- [16] D. Vantherin and D. M. Brink, Phys. Rev. C **3**, 626 (1972).
- [17] M. Beiner, H. Flocard, Nguyen Van Giai and P. Quentin, Nucl. Phys. A **238**, 29 (1975).
- [18] M. Dutra, O. Lourenco, A. Delfino, J. S. Sã Martins, C. Providência, S. S. Avancini and D. P. Menezes, Phys. Rev. C **77**, 035201 (2008).
- [19] N. Van Giai and H. Sagawa, Phys. Lett. B **106**, 379 (1981).
- [20] J. Bartel, P. Quentin, M. Brack, C. Guet and H. -B. Hakansson, Nucl. Phys. A **386**, 79 (1982).
- [21] M. Rayet, M. Arnould, F. Tondeur and G. Paulus, Astron. Astrophys. **116**, 183 (1982).
- [22] E. Chabanat, P. Bonche, P. Haensel, J. Meyer and R. Schaeffer, Nucl. Phys. A **635**, 231 (1998).
- [23] F. Tondeur, M. Brack, M. Farine and J. M. Pearson, Nucl. Phys. A **420**, 297 (1984).
- [24] B. K. Agrawal, S. Shlomo and V. K. Au, Phys. Rev. C **72**, 014310 (2005).
- [25] L. G. Cao, U. Lombardo, C. W. Shen and N. V. Giai, Phys. Rev. C **73**, 014313 (2006).
- [26] A. W. Steiner, M. Prakash, J. M. Lattimer and P. J. Ellis, Phys. Rep. **411**, 325 (2005).
- [27] L. Bennour, P. -H. Heenen, P. Bonche, J. Dobaczewski and H. Flocard, Phys. Rev. C **40**, 2834 (1989).
- [28] S. Weinberg, Physica A **96**, 327 (1979).
- [29] J. D. Walecka, Ann. Phys. (NY) **83**, 491 (1974).
- [30] J. Boguta and A. R. Bodmer, Nucl. Phys. A **292**, 413 (1977).
- [31] H. Georgi and A. Manohar, Nucl. Phys. B **234**, 189 (1984).
- [32] H. Georgi, Phys. Lett. B **298**, 187 (1993).
- [33] J. J. Rusnak and R. J. Furnstahl, Nucl. Phys. A **627**, 495 (1997).
- [34] R. J. Furnstahl and B. D. Serot, Nucl. Phys. A **671**, 447 (2000).
- [35] B. D. Serot, Lecture Notes in Physics, edited by Georgios A. Lalazissis, Peter Ring and Dario Vretenar, **641**, 31 (2004).
- [36] G. A. Lalazissis, J. Konig and P. Ring, Phys. Rev. C **55**, 540 (1997).
- [37] Y. Sugahara and H. Toki, Nuclear Physics A **579**, 557 (1994).
- [38] B. G. Todd-Rutel and J. Piekarewicz, Phys. Rev. Lett. **95**, 122501 (2005).
- [39] C. J. Horowitz and B. D. Serot, Nucl. Phys. A **368**, 503 (1981).
- [40] J. R. Oppenheimer and G. M. Volkoff, Phys. Rev. **55**, 374 (1939); R. C. Tolman, Phys. Rev. **55**, 364 (1939).

- [41] H. Komatsu, Y. Eriguchi and I. Hachisu, *Mon. Not. R. Astron. Soc.* **237**, 355 (1989).
- [42] N. K. Glendenning and F. Weber, *Phys. Rev. D* **50**, 3836 (1994).
- [43] N. Stergioulas and J. L. Friedman, *Astrophys. J.* **444**, 306 (1995).
- [44] Benjamin J. Owen, *Phys. Rev. L* **95**, 211101 (2005).
- [45] M. Bejger and P. Haensel, *Astron. Astrophys* **396**, 917 (2002).
- [46] P. Jaranowski, A. Krolak and B. F. Schutz, *Phys. Rev. D* **58**, 063001 (1998).
- [47] P. Danielewicz et al., *Science* **298**, 1592 (2002).
- [48] T. K. Jha and H. Mishra, *Phys. Rev. C* **78**, 065802 (2008).
- [49] F. J. Fattoyev, C. J. Horowitz, J. Piekarewicz and G. Shen, *Phys. Rev. C* **82**, 055803 (2010).
- [50] Plamen G. Krastev, Bao-An Li and Aaron Worley, *Phys. Lett. B* **668**, 1 (2008).
- [51] B. Haskell, N. Andersson, D. I. Jones and L. Samuelsson, *Phys. Rev. Lett.* **99**, 231101 (2007).